Differential Binding of Iron(III) and Zinc(II) Protoporphyrin IX to Synthetic Four-Helix Bundles

R. Eryl Sharp,† James R. Diers,‡ David F. Bocian,‡ and P. Leslie Dutton*,†

The Johnson Research Foundation
Department of Biochemistry and Biophysics
University of Pennsylvania
Philadelphia, Pennsylvania 19104
Department of Chemistry
University of California
Riverside, California 92521

Received February 9, 1998

Proteins containing metalloporphyrins support a diverse range of functions in biological systems.[1] Our immediate goal is to create simple synthetic protein-based structures using insights drawn from nature, which are capable of assembling, adopt a stable fold, and bind cofactors. Ultimately, we aim to construct molecular *maquettes*, which are functionalized synthetic protein versions of their biological counterparts.[2] To date, there has been much success with this approach, notably the incorporation of iron protoporphyrin IX (Fe-PP) into four-α-helix bundle proteins, via bis-histidine axial coordination to the porphyrin iron.[2−4] The Fe-PP maquettes can bind exogenous ligands such as cyanide and carbon monoxide, by displacing one of the coordinating axial histidines to the metal.[4] However, to engineer a binding site for exogenous ligands distal to the coordinated Fe-PP with a view to achieving catalysis, the Fe-PP must be five-coordinate, with the sixth coordination site vacant, or distal and easily accessible to substrate, as exemplified by cytochrome *c* peroxidase, cytochrome *c* oxidase, and the cytochromes P450.[5]

Herein we report the binding of Fe(III)-PP and Zn(II)-PP to two four-α-helix bundles, where the difference between the porphyrin coordination environment presented by the bundles and the preferred coordination geometry of the Zn(II)-PP and Fe(III)-PP is probed. Zn(II)-PP in noncoordinating solvents remains four-coordinate and in coordinating solvents or in the presence of good axial ligands, such as imidazole, tends to form five-coordinate complexes.[6] Fe(III)-PP on the other hand preferentially forms six-coordinate complexes in the presence of imidazole, although the protein environment can exert a strong influence on the actual nature of the axial coordination.[5] Our interest in Zn(II)-PP binding is further motivated by the fact that this complex is photoactivatable and would be useful for investigating light-initiated electron- and energy-transfer events between chromophores in multicofactor maquettes.[7] The present studies demonstrate that Zn(II)-PP binds to the synthetic proteins via single histidine axial ligation and that the binding affinity is remarkably high.

The peptides have the sequence Ac-L·KKLREEA·LKLLEEF·KKLLEE**X**·LKWLEGGGG-GGGGELLKL·**H**EELLKK·CEE-LLKL·AEERLKK·L-$CONH_2$, where **X** is either histidine or alanine and the dots in the sequence highlight the heptad repeat pattern of the helicies. The design was based on the prototype Fe-PP binding maquette,[2] except that each di-α-helical unit was synthesized as a continuous sequence to facilitate incorporation of different amino acids in the porphyrin axial coordination positions.[8] In αH22-l-αH41,[9] two histidines are present per di-α-helical unit to provide potential axial ligands to the porphyrins. However, in αA22-l-αH41, one of the histidines has been replaced with alanine, leaving a vacant sixth coordination site.

The secondary structure and the aggregation state of the assembled proteins without added porphyrin (apo maquettes) were investigated. Circular dichroic (CD) spectra of each protein had characteristic minima at 222 and 208 nm with a ratio $\Theta_{222}/\Theta_{208} \geq 1.0$, indicative of a coiled-coil α-helical structure,[2−4,10] and the intensity of the 222 nm signal corresponding to >70% helical content. Gel-permeation chromatography demonstrated that the peptides spontaneously self-assemble in aqueous solution to yield dimeric four-α-helix bundle proteins.[2−4] Both the secondary structure content and the aggregation state were invariant over the concentration range 0.1−100 μM.

The proteins were capable of binding Fe(III)-PP and Zn(II)-PP, characterized by a pronounced red shift in the porphyrin electronic absorption spectrum. The Fe(III/II)-PP bound to both bundle types and exhibited absorption features typical of low-spin *b*-type hemes (Fe(III)-PP γ_{max} at 411 and 535 nm, shifting on reduction to Fe(II)-PP to 424, 529, and 560 nm).[2−4] The Zn(II)-PP bound to both bundles also had absorption spectra similar to those of Zn(II)-PP-substituted natural cytochromes (γ_{max} at 425, 549, and 589 nm; $\epsilon_{425} \approx 250$ mM^{-1} cm^{-1}).[11] The secondary structure and aggregation state of the porphyrin containing holo maquettes were investigated to confirm that introduction of either Zn(II)-PP or Fe(III)-PP did not alter the four-α-helix bundle architecture. CD spectroscopy showed that the helicities of the apo and holomaquettes were the same within experimental error.[2−4] Gel-permeation chromatography revealed that, upon binding either Zn(II)-PP or Fe(III)-PP, >90% of the maquettes remained four-α-helix bundles,[2−4] with the remaining 10% present in higher aggregation states of six- and eight-α-helix bundles.

Careful titrations of Zn(II)-PP or Fe(III)-PP into [αH22-l-αH41]$_2$ showed that the binding stoichiometry was a maximum

* Corresponding author. Phone: (215) 898-8699. Fax: (215) 898-0465. E-mail: dutton@mail.med.upenn.edu.
† University of Pennsylvania.
‡ University of California, Riverside.

(1) (a) Chance, B.; Eastbrook, R. W.; Yonetani, T. *Heme Proteins*; Academic Press: New York, 1966. (b) Lemberg, R.; Barret, J. *Cytochromes*; Academic Press: New York, 1973.

(2) Robertson, D. E.; Farid, R. S.; Moser, C. M.; Urbauer, J. L.; Mulholland, S. E.; Pidikiti, R.; Lear, J. D.; Wand, A. J.; DeGrado, W. F.; Dutton, P. L. *Nature* **1994**, *368*, 425−432.

(3) (a) Choma, C. T.; Lear, J. D.; Nelson, M. J.; Dutton, P. L.; Robertson, D. E.; DeGrado, W. F. *J. Am. Chem. Soc.* **1994**, *116*, 856−865. (b) Kalsbeck, W. A.; Robertson, D. E.; Pandey. R. K.; Smith, K. M.; Dutton, P. L.; Bocian, D. F. *Biochemistry* **1996**, *35*, 3429−3428. (c) Gibney B. R.; Rabanal, F.; Skalicky, J. L.; Wand, A. J.; Dutton, P. L. *J. Am. Chem. Soc.* **1997**, *119*, 2323−2324. (d) Rabanal, F.; DeGrado, W. F.; Dutton, P. L. *J. Am. Chem. Soc.* **1996**, *118*, 473−474.

(4) Gibney, B. R.; Rabanal, F.; Reddy, K. S.; Dutton, P. L. *Biochemistry* **1998**, *37*, 4635−4643.

(5) (a) Moore G. R.; Pettigrew, G. W. *Cytochromes c: Evolutionary, Structural and Physiochemical Aspects*; Springer-Verlag: Berlin, New York, 1990. (b) Antonini, E.; Brunori, M. *Hemoglobin and Myoglobin in their Reactions with Ligands;* North-Holland: Amsterdam, 1971.

(6) (a) Ye, S.; Shen, C.; Cotton, T. M.; Kostic, N. M. *J. Inorg. Biochem.* **1997**, *65*, 219−226. (b) Feitelson, J.; Spiro, T. G. *Inorg. Chem.* **1986**, *25*, 5, 861−865. (c) Nappa, M.; Valentine, J. S. *J. Am. Chem. Soc.* **1978**, *100*, 5075−5080.

(7) (a) Koloczeck, H.; Horie, T.; Yonetani, H.; Anni, G.; Maniara, G.; Vanderkooi, J. M. *Biochemistry* **1987**, *26*, 3142−3148. (b) Zhou, J. S.; Kostic, N. M. *J. Am. Chem. Soc.* **1993**, *115*, 10796−10804. (c) Qin, L., Kostic, N. M. *Biochemistry* **1994**, *33*, 12592−12599.

(8) Peptides were assembled on a continuous flow solid-phase synthesizer using the fluorenylmethoxycarbonyl (Fmoc)/^{t}Bu strategy. Following chain assembly the peptides were N-terminal acetylated, washed with DMF and CH_2Cl_2, and then simultaneously cleaved and deprotected with trifluroacetic acid/ethanedithiol/water (90:8:2, v/v/v). Each peptide was purified to homogeneity by reversed-phase C_{18} HPLC and the molecular mass confirmed by laser desorption mass spectrometry. The cysteine present at position 48 for future covalent attachment of cofactors was blocked by reaction with a 10-fold molar excess of iodoacetamide. The amidylated peptides were purified to homogeneity by HPLC.

(9) α denotes the helical regions and l the flexible glycine linker between the helicies.

(10) Graddis, J. T.; Myszka, D. G.; Chaiken. I. M. *Biochemistry* **1993**, *32*, 12664−12671.

(11) (a) Anni, H.; Vanderkooi, J. M.; Mayne, L. *Biochemistry* **1995**, *34*, 5744−5753. (b) Chien, J. C. W. *J. Am. Chem. Soc.* **1977**, *100*, 1310−1312.

S0002-7863(98)00432-6 CCC: $15.00
Published on Web 07/03/1998

Table 1. Dissociation Constants for Fe(III)-PP and Zn(II)-PP Binding to Maquettes

	Fe(III)-PP		Zn(II)-PP	
maquette	K_D[a] (nM)	K_{D2} (nM)	K_{D1} (nM)	K_{D2} (nM)
$[\alpha H22\text{-l-}\alpha H41]_2$	35	135	30	90
$[\alpha A22\text{-l-}\alpha H41]_2$	23 000		<1	10

[a] The standard deviations in the reported K_D values are ±20%.

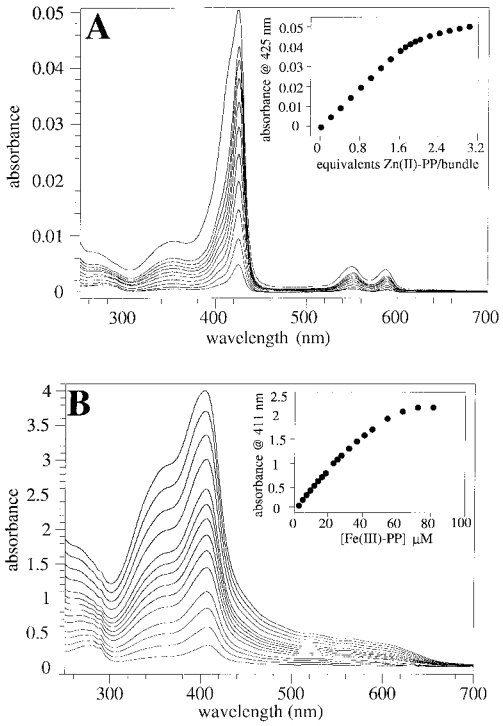

Figure 1. (A) UV−vis spectra in aqueous buffer (50 mM Tris, 100 mM NaCl, pH 8.0) of Zn(II)-PP titrated into 0.1 μM $[\alpha A22\text{-l-}\alpha H41]_2$. The molar equivalents of Zn(II)-PP added per bundle in increasing absorbance intensity are 0.2, 0.4, 0.6, 0.8, 1.0, 1.2, 1.4, 1.6, 1.8, 2.0, and 3.0 (for the last titer, the shoulder to the blue of the Soret absorption is due to unbound Zn(II)-PP). The inset shows a plot of the increase in the Soret absorption of Zn(II)-PP upon binding to $[\alpha A22\text{-l-}\alpha H41]_2$ against the molar ratio of Zn(II)-PP per bundle. (B) UV−vis spectra in aqueous buffer of Fe(III)-PP titrated into 22.4 μM $[\alpha H22\text{-l-}\alpha H41]_2$. The molar equivalents of Fe(III)-PP added per bundle in increasing absorbance intensity are 0.2, 0.4, 0.6, 0.8, 1.0, 1.2, 1.4, 1.6, 1.8, 2.0, 2.4, 2.8, and 3.2 (the large shoulder to the blue of the Soret absorption and the apparent blue shift in the Soret maximum for titers ≥0.6 molar equivalents Fe(III)-PP per bundle is due to unbound Fe(III)-PP). The inset shows a plot of the calculated absorption at 411 nm due to the bound Fe(III)-PP (contributions from bound and free Fe(III)-PP were calculated using a spectral deconvolution fitting procedure) against the concentration of Fe(III)-PP titrated.

of two Fe(III)-PP or two Zn(II)-PP molecules per four-α-helix bundle; that is, each bis-histidine coordination site bound one Zn(II)-PP or Fe(III)-PP. Table 1 shows that the K_D values for binding of the two Fe(III)-PP were ∼35 and 135 nM, almost identical to previously reported values for similar maquettes.[4] The K_D values for binding of the two Zn(II)-PP to $[\alpha H22\text{-1-}\alpha H41]_2$ were also nanomolar (Table 1). The binding stoichiometry for Zn(II)-PP to $[\alpha A22\text{-l-}\alpha H41]_2$ was also 2:1, with the first K_D in the subnanomolar range and the second $K_D \approx 10$ nM (Table 1, Figure 1), indicating that a single axial histidine is sufficient for tight binding of Zn(II)-PP to each di-α-helical unit. The failure of more than two Zn(II)-PP maquettes to bind to the four histidines present in $[\alpha H22\text{-l-}\alpha H41]_2$ is probably due to the fact that binding of more than one Zn(II)-PP to each di-α-helical unit would severely compromise bundle stability. In the case of Fe(III)-PP binding to $[\alpha A22\text{-l-}\alpha H41]_2$, the stoichiometry was 1:1, with a $K_D \approx 23$ μM (Table 1, Figure 1), which is $>2 \times 10^3$ fold larger in magnitude than the K_D for binding of the second Zn(II)-PP to the same bundle. Thus, by replacing one of the coordinating histidines in each di-α-helical unit by alanine, the specificity of Zn(II)-PP binding over Fe(III)-PP is enhanced by at least 3 orders of magnitude. In $[\alpha A22\text{-l-}\alpha H41]_2$, the bound Fe(III)-PP must adopt a bis-histidine ligation geometry between the single histidines present on each $[\alpha A22\text{-l-}\alpha H41]$ monomer (Figure 2), which is energetically unfavorable because a conformational change in the bundle is required to effectively bind Fe(III)-PP in this manner. This explains the observed stoichiometry and low binding affinity. It is clear that Fe(III)-PP binding to $[\alpha A22\text{-l-}\alpha H41]_2$ by five-coordinate single axial histidine ligation is significantly less favorable than bis-histidine ligation across two $[\alpha A22\text{-l-}\alpha H41]$ monomers by ∼4 kcal mol^{-1}.

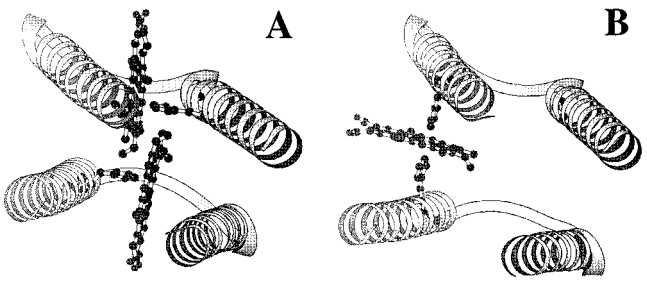

Figure 2. Molecular graphic ribbon representation of the $[\alpha A22\text{-l-}\alpha H41]_2$ maquette: (A) two Zn(II)-PP molecules bound by a single axial histidine ligand in each di-α-helical unit; (B) one Fe(III)-PP molecule bound by intermonomer bis-histidine ligation between the single histidines present on each di-α-helical unit of the four-α-helix bundle.

The coordination geometries of Fe(III)-PP and Zn(II)-PP in both $[\alpha H22\text{-l-}\alpha H41]_2$ and $[\alpha A22\text{-l-}\alpha H41]_2$ were investigated by resonance Raman (RR) spectroscopy.[12] The RR spectra of both Fe(III)-PP maquettes are characteristic of bis-histidine ligated species, are similar to one another, and resemble previously reported RR spectra for other Fe(III)-PP maquettes.[3b] The RR spectra of both Zn(II)-PP maquettes are also similar to one another and are analogous to imidazole-coordinated Zn(II)-PP in solution and Zn(II)-PP reconstituted into myoglobin.[6b] In addition, the RR spectra of both Zn(II)-PP maquettes exhibit a broad feature at ∼158 cm^{-1} that is absent from the spectrum of four-coordinate Zn(II)-PP in solution.[6b] This band is attributed to the Zn−His stretching vibration by analogy to the assignment of this mode in Zn(II)-PP myoglobin. In the latter protein, the Zn−His stretch occurs at ∼148 cm^{-1}. Accordingly, the strength of the Zn−His bond is similar for the Zn(II)-PP maquette and Zn(II)-PP myoglobin.

The studies reported herein demonstrate that metalloporphyrin axial coordination in the synthetic protein architectures is governed by the preferred geometry of the metal ion (Fe(III/II), six-coordinate; Zn(II), five-coordinate). In contrast, certain natural heme proteins provide an environment that readily accommodates the highly unfavorable five-coordinate state of the iron ion.[1] This feature of the natural proteins illustrates the exquisite tailoring of the heme binding site required for achieving efficacious biological activity.

Acknowledgment. R.E.S. acknowledges the receipt of a postdoctoral fellowship from the North Atlantic Treaty Organization (NATO). This work was supported by NIH Grants GM41048 (P.L.D.) and GM36243 (D.F.B.). Mass spectrometry analysis was performed by the University of Pennsylvania Protein Chemistry Laboratory. We thank Dr. Kim Sharp for assistance in preparing Figure 2.

Supporting Information Available: Resonance Raman spectra of the Fe(III)-PP and Zn(II)-PP bound to $[\alpha H22\text{-l-}\alpha H41]_2$ and $[\alpha A22\text{-l-}\alpha H41]_2$ (4 pages, print/PDF). See any current masthead page for ordering information and Web access instructions.

JA980432Y

(12) The RR spectra were recorded using instrumentation and procedures previously described.[3b] The sample concentrations were typically 50−100 μm. The excitation wavelength was 415.4 nm, and the laser powers was ∼5 mW.